NASA TECHNICAL NOTE

NASA TN D-4640

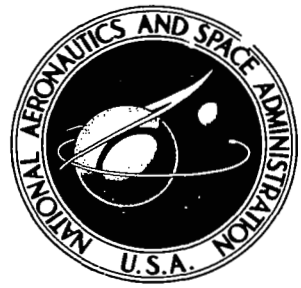

MAXIMUM DROP DIAMETERS FOR THE ATOMIZATION OF LIQUID JETS INJECTED COCURRENTLY INTO ACCELERATING OR DECELERATING GAS STREAMS

by Robert D. Ingebo

Lewis Research Center
Cleveland, Ohio

NATIONAL AERONAUTICS AND SPACE ADMINISTRATION • WASHINGTON, D. C. • JULY 1968

NASA TN D-4640

MAXIMUM DROP DIAMETERS FOR THE ATOMIZATION OF LIQUID JETS INJECTED COCURRENTLY INTO ACCELERATING OR DECELERATING GAS STREAMS

By Robert D. Ingebo

Lewis Research Center
Cleveland, Ohio

NATIONAL AERONAUTICS AND SPACE ADMINISTRATION

For sale by the Clearinghouse for Federal Scientific and Technical Information
Springfield, Virginia 22151 – CFSTI price $3.00

ABSTRACT

The determining effect of six dimensionless groups on the maximum drop-diameter was studied for the atomization of jets of ethanol or water injected into nitrogen or helium gas streams cocurrently or into still air. Values of the ratio of orifice diameter to maximum drop-diameter D_o/D_m were obtained from photomicrographs of the sprays and related to the dimensionless groups as follows:

$$\frac{D_o}{D_m} = f(Bo, Re_L, Re_g, We_L, We_g, Ac)$$

where Bo is the ratio of hydrostatic to surface-tension forces and Ac is an aerodynamic-acceleration to surface-tension ratio. Re_L, Re_g, We_L, and We_g are the liquid-jet and gas-stream Reynolds and Weber numbers, respectively. Liquid-injection velocities covered a range of nearly 0 to 6250 cm/sec. Gas-stream velocities were varied from the still-air condition to helium-gas velocities of 14 000 cm/sec. Gas-stream accelerations ranged from 833 000 to 19 200 000 cm/sec^2, and decelerations of 672 000 to 4 880 000 cm/sec^2.

STAR Category 12

MAXIMUM DROP DIAMETERS FOR THE ATOMIZATION OF LIQUID JETS INJECTED COCURRENTLY INTO ACCELERATING OR DECELERATING GAS STREAMS

by Robert D. Ingebo

Lewis Research Center

SUMMARY

Maximum drop-diameters were obtained from photomicrographs of atomized jets of ethanol or water injected into nitrogen or helium gas-streams cocurrently or into still air. They were used to characterize the fineness of atomization by means of the ratio of orifice diameter to maximum drop-diameter D_o/D_m. This dimensionless ratio was correlated with six dimensionless groups used as criteria for liquid jet instability in the following expression

$$\frac{D_o}{D_m} = f(Bo, Re_L, Re_g, We_L, We_g, Ac)$$

where Bo is the ratio of hydrostatic- to surface-tension forces and Ac is an aerodynamic-acceleration to surface-tension ratio. Re_L, Re_g, We_L, and We_g are the liquid-jet and gas-stream Reynolds and Weber numbers, respectively.

Analysis of the data gave the following expression:

$$\frac{D_o}{D_m} = 0.64\left(\frac{D_o}{D_t}\right)^{0.33} Bo^{0.33} + Re_L^{-0.1} Re_g^{0.5} Bo^{-0.07}$$

$$\times \left[0.044 + We_L We_g^{-0.2} Bo^{-0.07}(1.25\times10^{-6} + 3.3\times10^{-5} Ac^{0.5} Bo^{-0.66})\right]$$

which was compared with the results of other investigations of the atomization of cocurrent liquid-jets in constant-velocity gas streams. Some of the exponents for individual fluid properties were found to be in reasonably good agreement with those determined in this investigation.

In this study, liquid-jet injection velocities were varied from nearly zero velocity up to 6250 centimeters per second. Gas-stream velocities ranged from the still-air condition to 458 feet per second for helium gas streams. Gas-stream acceleration rates were varied from 833 000 to 19 200 000 centimeters per second squared and deceleration rates from 672 000 to 4 880 000 centimeters per second squared.

INTRODUCTION

The aerodynamic force of a gas stream is one of the most important factors known in determining the degree of fineness of atomization of liquid jets (ref. 1). Thus, it is a determining factor in obtaining completeness of combustion of liquid fuels in turbojet afterburners and rocket combustors (refs. 2 and 3). However, at present, very little is known about the aerodynamic effect of accelerating or decelerating combustion-gases on the atomization of fuel jets. Thus, the purpose of this study was to simulate combustor conditions by accelerating or decelerating gas streams in a variable area duct to determine this effect on the fineness of atomization.

In the first part of this investigation, drop formation was studied by slowly dripping ethanol or water into still air. This provided a reference condition in which only one dimensionless group was used as a criteria for liquid-jet instability. In the remaining portion of the study, the effects of additional dimensionless groups were investigated. First, the liquid-jet velocity was set equal to the gas-stream velocity. Next, a relatively high velocity difference was maintained between the liquid jet and the gas stream. Finally, the effect of an accelerating or decelerating gas stream was investigated.

Photomicrographs of the drops were obtained with a high-speed camera developed at the Lewis Research Center (ref. 4). The maximum drop-diameter was then determined from the photomicrographs and correlated with dimensionless groups which were systematically increased from one, in the initial correlation, to six in the final analysis. From this analysis, it was possible to determine the effect of gas-stream acceleration or deceleration on the fineness of atomization of liquid-jets injected cocurrently into gas streams.

For this investigation, fineness of atomization was characterized by the ratio of orifice diameter to maximum drop-size D_o/D_m. This ratio was chosen for ease in analysis rather than its reciprocal D_m/D_o. Other investigators (refs. 5 and 6) have used the mass-median drop size or the Sauter mean-diameter (ref. 7) to characterize atomization. However, there were no data available on maximum drop-sizes for accelerating gas streams. Thus, direct comparison could not be made with the main results of this study. However, exponents for individual fluid-properties could be compared qualitatively.

EXPERIMENTAL PROCEDURE

In the initial portion of this study, the test-section shown in figure 1 was used at atmospheric pressure to determine liquid-jet breakup in still air and in constant velocity gas streams. The test section shown in figure 2 was used at atmospheric pressure to determine the effect of gas-stream acceleration forces on the atomization process. In the case of decelerating gas flow, the test section was inverted and the gas-manifold

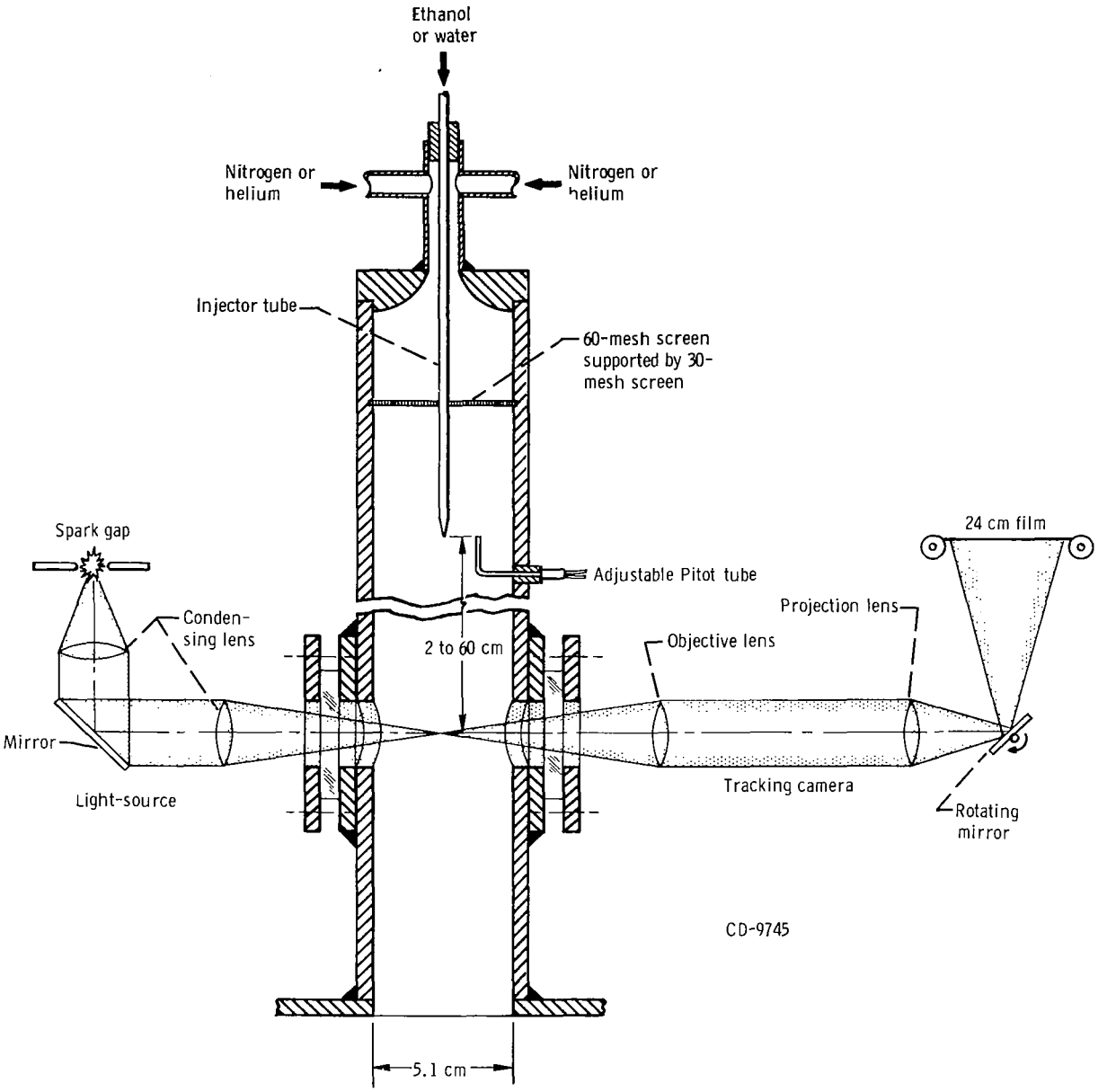

Figure 1. - Experimental equipment for studying liquid-jet atomization in still air and constant-velocity gas streams.

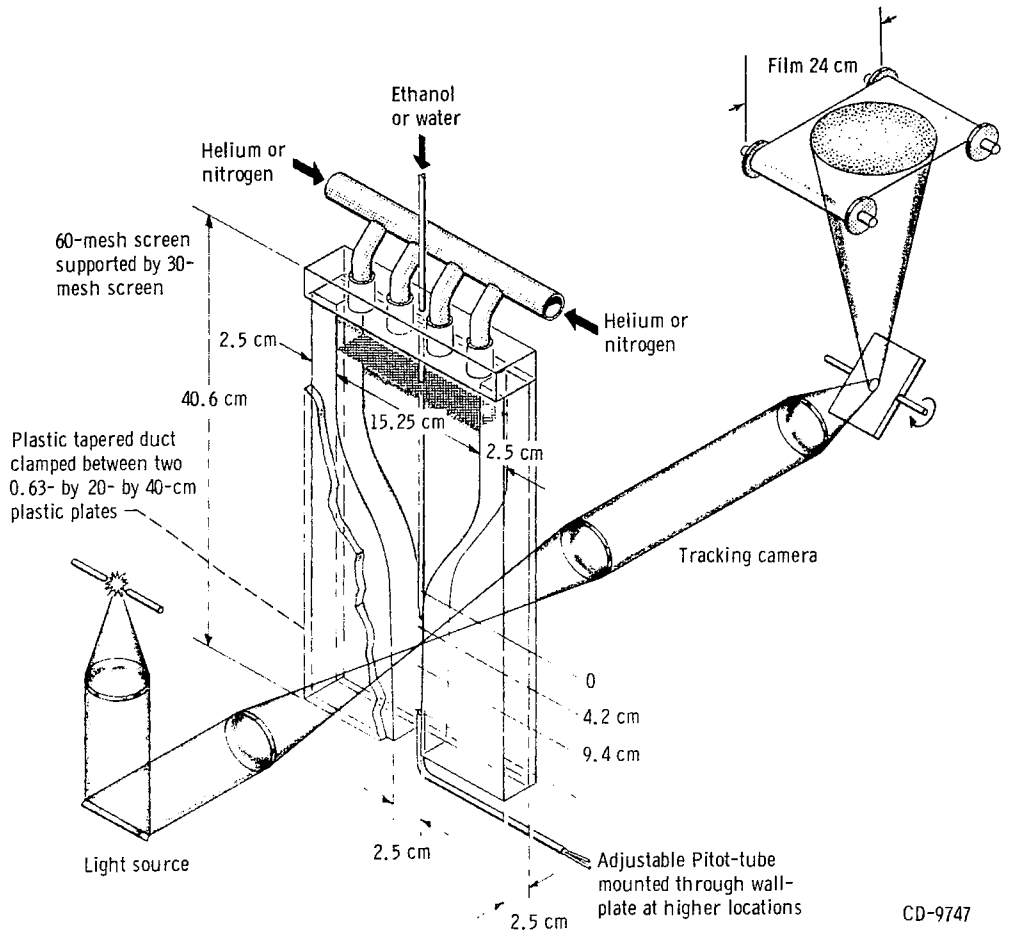

Figure 2. - Experimental equipment for determining effect of gas-stream acceleration on liquid-jet atomization.

section was removed. Gas flow and the injector tube were admitted through the 1-inch square opening in the test section.

The test section shown in figure 2 was designed to give constant gas-stream acceleration as shown by the data plotted in figure 3. The acceleration of the gas stream ($a = 1/2\ dV_g^2/dx$) was obtained from the slope of the lines plotted for four different mass flow conditions. Thus, it was possible to obtain four different acceleration rates at approximately the same gas-stream velocity condition, as noted by the dashed line in figure 3. Each data point was obtained with the pitot tube located at each of the liquid-injection stations.

The test liquid, ethanol or water, was injected through a 2.54-centimeter length of stainless steel tubing inserted in the injector-tube holder as shown in figure 4. The inside diameter D_o of the tube was varied from 0.0254 to 0.1678 centimeter and the liquid was allowed to slowly drip into still air or injected into gas streams of nitrogen and he-

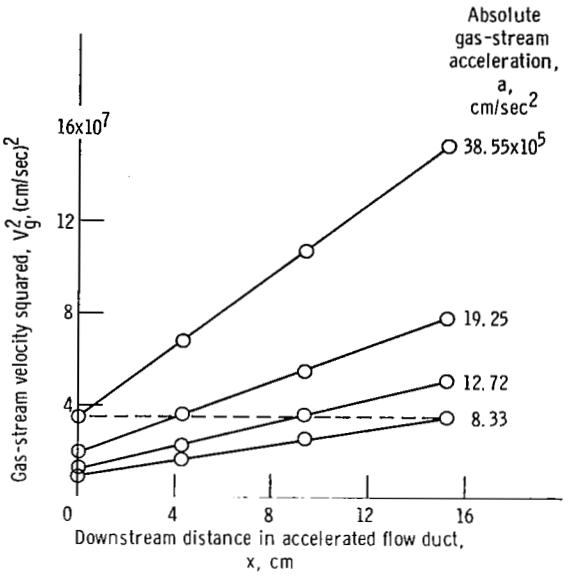

Figure 3. - Gas-stream acceleration data.

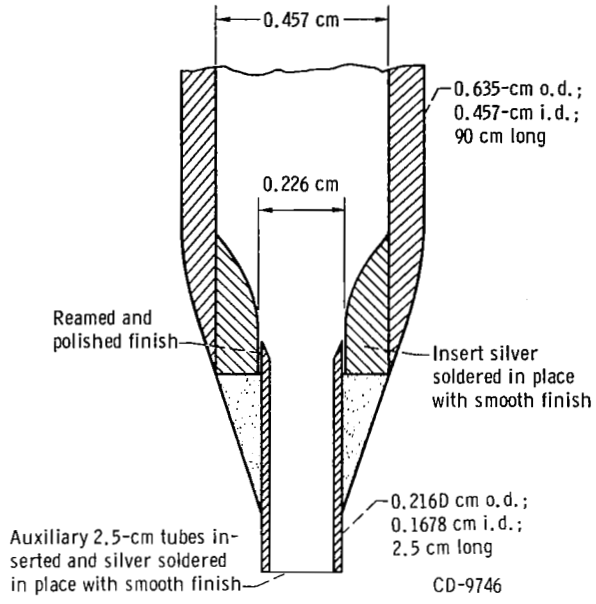

Figure 4. - Diagram of injector-tube detail. (See table II.)

TABLE I. - FLUID PROPERTIES AT ATMOSPHERIC PRESSURE AND 20° C

Fluid	Density, g/cm^3	Viscosity, N-sec/m^2	Surface tension, N/cm
Gas:			
Nitrogen	11.70×10^{-4}	1.81×10^{-5}	-------
Helium	1.67	1.99	-------
Liquid:			
Ethanol	0.79	1.194×10^{-3}	23×10^{-5}
Water	1.00	1.009	73

lium. Properties of the fluids are given in table I.

Photomicrographs of the drops were obtained at a magnification of 22 diameters with a high-speed camera developed at the Lewis Research Center. This camera is described in detail in reference 3. The maximum drop-diameter D_m was measured directly from contact prints with an eye piece having small scale subdivisions of 0.10 millimeter which gave drop measurements that were reproducible within ±5 microns. Only drop images that were in sharp focus were measured, and a minimum of 10 photomicrographs were used to determine the maximum drop-diameter for each test condition. Data for all of the tests are given in table II.

TABLE II. - TEST CONDITIONS, MAXIMUM DROP-DIAMETERS, AND DIMENSIONLESS GROUPS

Orifice diameter, D_o, cm	Tip diameter, D_t, cm	Maximum drop diameter, D_m, cm	Liquid velocity, V_l, cm/sec	Gas velocity, V_g, cm/sec	Velocity difference, ΔV, cm/sec	Gas-stream acceleration, a_g, cm/sec^2	Bond number, Bo	Liquid-film Reynolds number, Re_L	Gas-stream Reynolds number, Re_g	Liquid-film Weber number, We_L	Gas-stream Weber number, We_g	Aerodynamic acceleration to surface-tension force ratio, Ac
Ethanol in still air												
0.0254	0.0483	0.1800	----	----	------	----------	0.022	------	----	-------	------	------
.0610	.1070	.2280	----	----	------	----------	.125	------	----	-------	------	------
.1016	.1620	.2660	----	----	------	----------	.347	------	----	-------	------	------
.1678	.2160	.2800	----	----	------	----------	.948	------	----	-------	------	------
Water in still air												
0.0254	0.0483	0.2500	----	----	------	----------	0.0087	------	----	-------	------	------
.0610	.1070	.3050	----	----	------	----------	.0500	------	----	-------	------	------
.1016	.1620	.3600	----	----	------	----------	.1386	------	----	-------	------	------
.1678	.2160	.4000	----	----	------	----------	.3780	------	----	-------	------	------
Ethanol in nitrogen gas stream												
0.0254	0.0483	0.0300	5700	5700	------	----------	0.022	9 585	936	-------	------	------
		.0360	3720	3720	------	----------		6 253	611	-------	------	------
		.0370	3050	3050	------	----------		5 126	501	-------	------	------
		.0380	2470	2470	------	----------		4 152	406	-------	------	------
		.0440	1680	1680	------	----------		2 819	275	-------	------	------
		.0480	1220	1220	------	----------		2 050	200	-------	------	------
		.0580	610	610	------	----------	↓	1 025	100	-------	------	------
0.0610	0.1070	0.0520	5490	5490	------	----------	0.125	22 158	2165	-------	------	------
		.0640	3720	3720	------	----------		15 018	1467	-------	------	------
		.0680	2560	2560	------	----------		10 340	1010	-------	------	------
		.0940	1555	1555	------	----------		6 278	613	-------	------	------
		.1100	915	915	------	----------	↓	3 693	361	-------	------	------
0.1016	0.1620	0.0740	5270	5270	------	----------	0.347	35 470	3465	-------	------	------
		.0800	4420	4420	------	----------		29 729	2904	-------	------	------
		.0920	2990	2990	------	----------		20 093	1963	-------	------	------
		.1650	885	885	------	----------	↓	5 741	561	-------	------	------
0.1678	0.2160	0.1070	3990	3990	------	----------	0.948	44 307	4329	-------	------	------
		.1200	1860	1860	------	----------	.948	20 631	2016	-------	------	------
Water in nitrogen gas stream												
0.0254	0.0483	0.0320	5150	5150	------	----------	0.00866	12 976	846	-------	------	-------
		.0340	4120	4120	------	----------		10 365	676	-------	------	-------
		.0380	3420	3420	------	----------		8 599	561	-------	------	-------
		.0408	2290	2290	------	----------		5 758	376	-------	------	-------
		.0640	610	2290	------	----------	↓	1 536	100	-------	------	-------
Ethanol in helium gas stream												
0.0254	0.0483	0.0620	6250	6250	------	----------	0.022	10 508	133	-------	------	-------
		.0650	4880	4880	------	----------		8 201	104	-------	------	-------
		.0715	3050	3050	------	----------		5 126	65	-------	------	-------
		.0890	1525	1525	------	----------	↓	2 563	33	-------	------	-------

TABLE II. - Concluded. TEST CONDITIONS, MAXIMUM DROP-DIAMETERS, AND DIMENSIONLESS GROUPS

Orifice diameter, D_o, cm	Tip diameter, D_t, cm	Maximum drop diameter, D_m, cm	Liquid velocity, V_l, cm/sec	Gas velocity, V_g, cm/sec	Velocity difference, ΔV, cm/sec	Gas-stream acceleration, a_g, cm/sec^2	Bond number, Bo	Liquid-film Reynolds number, Re_L	Gas-stream Reynolds number, Re_g	Liquid-film Weber number, We_L	Gas-stream Weber number, We_g	Aerodynamic acceleration to surface-tension force ratio, Ac
Ethanol in nitrogen gas stream												
0.0254	0.0483	0.0310	2440	3 965	1 525	----------	0.022	4100	651	2 029	3.01	------
		.0245	2440	5 490	3 050	----------		4100	901	8 116	12.02	------
		.0160	2440	8 540	6 100	----------		4100	1402	32 463	48.08	------
		.0350	975	2 500	1 525	----------		1640	411	2 029	3.01	------
		.0260	↓	4 025	3 050	----------		↓	661	8 116	12.02	------
		.0160		7 075	6 100	----------			1162	32 463	48.08	------
		.0115		9 150	8 175	----------			1502	58 291	86.33	------
		.0360	488	2 013	1 525	----------		820	331	2 029	3.01	------
		.0260	488	3 538	3 050	----------		820	581	8 116	12.02	------
		.0195	488	5 063	4 575	----------	↓	820	831	18 261	27.04	------
Ethanol in helium gas stream												
0.0254	0.0483	0.0365	488	5 917	5 429	----------	0.022	820	126	25 714	5.43	------
		.0260	488	8 083	7 595	----------	.022	820	172	50 319	10.60	------
		.0170	488	10 858	10 370	----------	.022	820	232	93 819	19.80	------
0.0508	0.0810	0.0310	366	8 083	7 717	----------	0.087	1230	345	103 897	21.90	------
		.0210	366	10 858	10 492	----------	.087	1230	462	192 078	40.50	------
		.0170	366	12 200	11 834	----------	.087	1230	520	244 357	51.50	------
0.1016	0.1620	0.0300	244	8 113	7 869	----------	0.347	1640	692	216 088	45.60	------
		.0200	244	12 322	12 078	----------	.347	1640	1050	509 075	107.30	------
Ethanol with nitrogen gas-stream acceleration												
0.0254	0.0483	0.0146	488	5 887	5 399	8.33×10^5	0.022	820	966	25 426	37.7	0.0273
		.0140	↓	6 009	5 521	12.72	↓	↓	986	26 588	39.4	.0417
		.0135		5 917	5 429	19.25			972	25 714	38.1	.0632
		.0128		5 917	5 429	38.55			972	25 714	38.1	.1265
0.0508	0.0810	0.0198	366	5 887	5 521	8.33×10^5	0.087	1230	1933	53 176	78.8	0.1093
		.0192	↓	6 009	5 643	12.72	↓	↓	1973	55 553	82.3	.1670
		.0183		5 917	5 551	19.25			1943	53 766	79.6	.2527
		.0171		5 917	5 551	38.55			1943	53 766	79.6	.5061
0.1016	0.1620	0.0235	244	5 887	5 643	8.33×10^5	0.347	1640	3866	111 105	164.5	0.4372
		.0230	↓	6 009	5 765	12.72	↓	↓	3946	115 962	171.7	.6679
		.0220		5 917	5 673	19.25			3886	112 310	166.3	1.0106
		.0200		5 917	5 673	38.55			3886	112 310	166.3	2.0244
0.1678	0.2160	0.0265	153	5 887	5 734	8.33×10^5	0.948	1695	6377	189 273	280.3	1.1898
		.0250	↓	6 009	5 856	12.72	↓	↓	6509	197 412	292.4	1.8173
		.0245		5 917	5 764	19.25			6410	191 291	283.3	2.7500
		.0235		5 917	5 764	38.55			6410	191 291	283.3	5.5080
Water with nitrogen gas-stream acceleration												
0.0254	0.0483	0.0175	488	5 917	5 429	12.72×10^5	0.00866	1228	972	10 255	12.0	0.0132
		.0220	1830	5 917	4 087	12.72	.00866	4607	972	5 812	6.8	.0132
		.0245	286	5 917	3 101	12.72	.00866	7064	972	3 368	3.9	.0132
Ethanol with helium gas-stream acceleration												
0.1016	0.1620	0.0110	244	13 969	13 725	51.55×10^5	0.347	1640	1190	657 380	139.0	0.3863
		.0100	↓	↓	13 725	69.24	↓	↓	↓	↓	↓	.5189
		.0095			13 725	108.89						.8161
		.0090			13 725	192.15						1.4402
Ethanol with nitrogen gas-stream deceleration												
0.0254	0.0483	0.0195	488	4 514	4 026	6.71×10^5	0.022	820	741	14 141	20.9	0.0220
		.0160	↓	5 490	5 002	9.15	↓	↓	901	21 828	32.3	.0300
		.0075		8 540	8 052	29.89			1402	56 564	83.8	.0981
		.0042		11 285	10 797	48.80			1853	101 704	150.6	.1602

ANALYSIS

The fineness of atomization of a liquid jet in a gas stream may be characterized by the nondimensional ratio of the orifice diameter to the maximum drop-diameter D_o/D_m. For ease of analysis, this ratio was used instead of its reciprocal D_m/D_o which was used in reference 1. In order to evaluate the ratio D_o/D_m, it may be assumed to be a function of six dimensionless groups as follows:

$$\frac{D_o}{D_m} = f(Bo, Re_L, Re_g, We_L, We_g, Ac) \tag{1}$$

Each dimensionless group was based on the orifice diameter as the characteristic length, and defined in the following manner:

Gravitational-acceleration Bond number Bo

The gravitational-acceleration Bond number Bo (ref. 8) indicates the degree of instability of a liquid jet acted upon by a hydrostatic pressure force. It is based on the acceleration due to gravity g.

$$Bo = \frac{\rho_l D_o^2 g}{\sigma} \tag{2}$$

where ρ_l is the liquid density and σ is the surface tension.

Liquid-jet Reynolds number Re_L

The liquid-jet Reynolds number Re_L indicates the degree of turbulence of a liquid flowing in an injector tube.

$$Re_L = \frac{\rho_l D_o V_l}{\mu_l} \tag{3}$$

where V_l and μ_l are the liquid velocity and viscosity, respectively.

Gas-stream Reynolds number Re_g

The gas-stream Reynolds number Re_g indicates the degree of turbulence of a gas stream flowing parallel with an injector tube.

$$Re_g = \frac{\rho_g D_o V_g}{\mu_g} \tag{4}$$

where ρ_g, V_g, and μ_g are the gas density, velocity, and viscosity, respectively.

Gas-stream Weber number We_g

The gas-stream Weber number We_g indicates the degree of instability of a liquid jet acted upon by a stagnation pressure force. It is based on gas density and the absolute velocity difference between the liquid jet and the gas stream.

$$We_g = \frac{\rho_g D_o (V_g - V_l)^2}{\sigma} \tag{5}$$

Liquid-jet Weber number We_L

The liquid-jet Weber number We_L indicates the degree of instability of a liquid jet in a manner similar to that of the gas-stream Weber number. It is based on liquid density and the absolute velocity difference between the liquid jet and the gas stream

$$We_L = \frac{\rho_l D_o (V_g - V_l)^2}{\sigma} \tag{6}$$

Aerodynamic-acceleration group Ac

The aerodynamic-acceleration group Ac indicates the degree of instability of a liquid jet due to the additional effects present with an accelerating or decelerating gas stream. It is based on the absolute acceleration of the gas stream a.

$$Ac = \frac{\rho_g D_o^2 a}{\sigma} \tag{7}$$

Relations between the dimensionless groups used in the analysis of the data are illustrated in figure 5. Solid lines in the figure indicate the groups that were used and dashed lines indicate other possible groups. In order to determine the effect of the dimensionless groups on the maximum drop-diameter, as indicated in equation (1), the first case considered was that in which the hydrostatic-pressure and surface-tension forces control the atomization process.

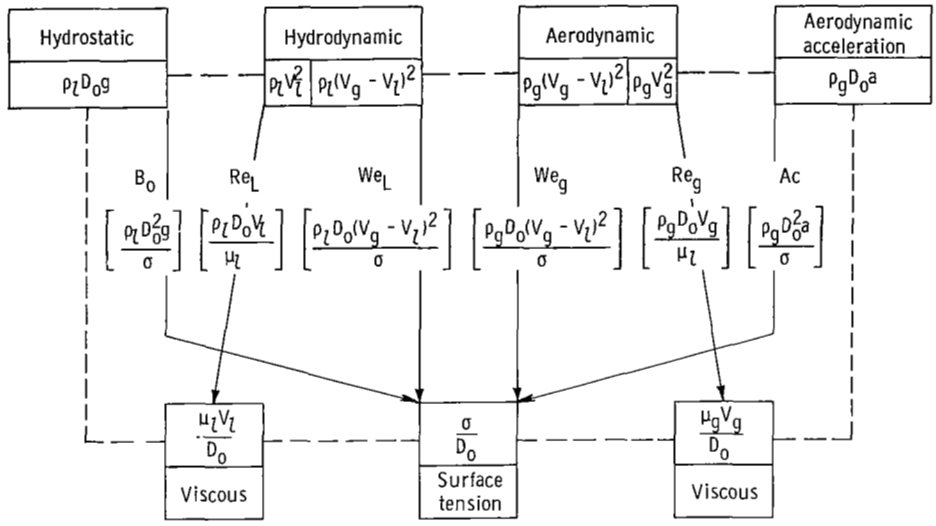

Figure 5. - Relations between dimensionless groups based on orifice diameter as characteristic length. (Dashed lines indicate other possible combinations.)

Gravitational Force Controlling Liquid-Jet Atomization

When a drop is gently released into still air, then $V_l \approx 0$ and the following force balance may be written as a limiting condition for the maximum drop-diameter:

Gravitational force = Surface-tension force

or

$$g \frac{1}{6} \rho_l \pi D_m^3 = \pi D_t \sigma \psi \tag{8}$$

where ψ is a proportionality constant and D_t is the tip or outside diameter of the injector tube. Rewriting equation (8) gives:

$$\frac{\rho_l D_m^3 g}{6 D_t \sigma} = \psi \tag{9}$$

Thus, ψ is a gravitational- to surface-tension force ratio and appears to be quite similar to the Bond number defined by equation (2). However, the diameter terms are quite different in the two expressions.

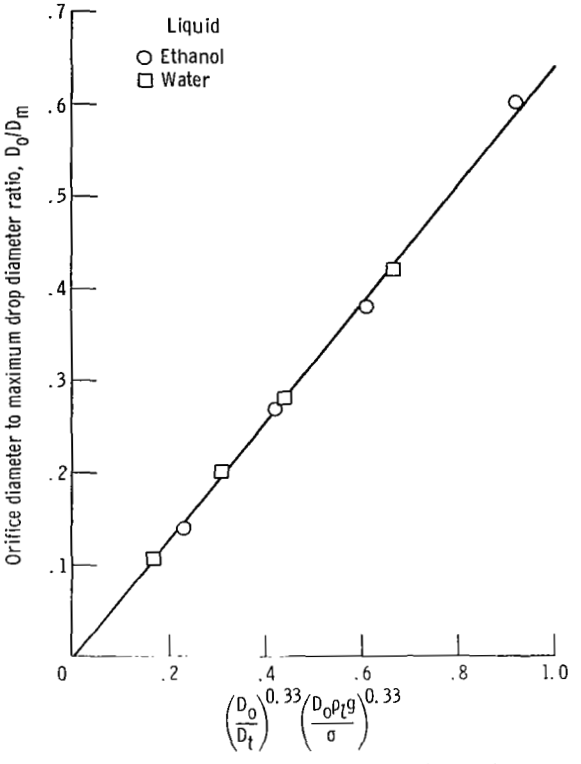

Figure 6. - Effect of gravitational acceleration on liquid-jet atomization. Liquid jet velocity, 0; gaseous environment, still air.

In order to obtain an expression that could be related to equation (1) both sides of equation (9) may be multiplied by $(D_o/D_m)^3$ which gives the following relation

$$\frac{D_o}{D_m} = (6\psi)^{-0.33}\left(\frac{D_o}{D_t}\right)^{0.33} Bo^{0.33}$$

since $Bo = \rho_l D_o^2 g/\sigma$ as defined by equation (2). By plotting the experimental data for D_o/D_m against the product $(D_o/D_t)^{0.33}Bo^{0.33}$ (as shown in fig. 6) the following expression was obtained:

$$\frac{D_o}{D_m} = 0.64\left(\frac{D_o}{D_t}\right)^{0.33} Bo^{0.33} \tag{10}$$

where Bo is a hydrostatic- to surface-tension force ratio based on the characteristic length D_o as shown in the chart of dimensionless groups in figure 5. The constant 0.64

in equation (10) corresponds to a value of 0.635 for ψ, which is in good agreement with reference 9 and other studies of pendant drops.

Fluid Dynamic Forces Controlling Atomization

In order to determine the effect of the other five dimensionless groups given in equation (1), three conditions were considered in which fluid dynamic forces controlled the atomization process. First, the gas-stream and liquid-jet velocities were set equal. Next, a relatively high velocity difference was maintained between the gas stream and the liquid jet. Finally, the effect of accelerating or decelerating the gas stream was determined.

Free-stream gas velocity and free-stream jet velocity are equal and constant. - For this condition, $V_g = V_l$, $We_L = 0$, $We_g = 0$, and $Ac = 0$. Thus, in order to include the additional effect of the liquid and gas Reynolds numbers, the following form of equation (1) was chosen as a modification of equation (10):

$$\left(\frac{D_o}{D_m} - \beta_1\right) = bRe_g^m Re_L^n Bo^p \tag{11}$$

where

$$\beta_1 = 0.64\left(\frac{D_o}{D_t}\right)^{0.33} Bo^{0.33}$$

as in equation (10).

Since Re_g and Re_L could not be varied independently, it was necessary to determine exponents for Re_g and the ratio Re_g/Re_L. From these results, the values of the exponents m and n in equation (11) could be determined. Similarly, plotting the data against Re_L and the ratio Re_L/Re_g, gave the same values for the exponents m and n. Thus, from the slopes of the plots in figures 7 and 8, the following relation was obtained:

$$\left(\frac{D_o}{D_m} - \beta_1\right) \sim Re_g^{0.4}\left(\frac{Re_g}{Re_L}\right)^{0.1} \sim Re_g^{0.5} Re_L^{-0.1}$$

The proportionality constant b and the exponent p in equation (11) were evaluated from the data plot shown in figure 9. This gave the following expression for equation (11):

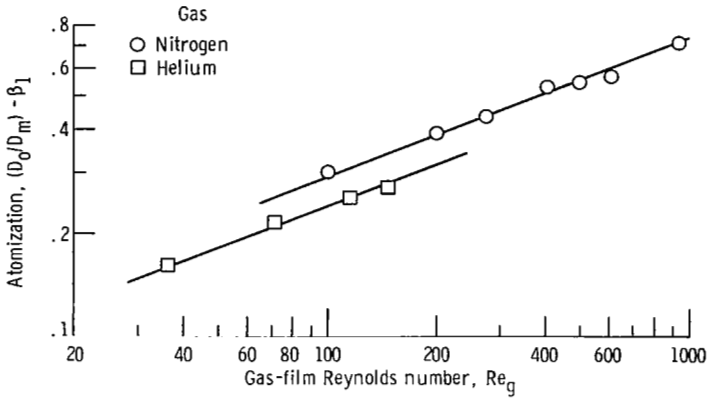

Figure 7. - Effect of gas-film Reynolds number on atomization, with liquid-film Reynolds number varying. Slope, 0.4; liquid, ethanol; orifice diameter, 0.025 centimeter.

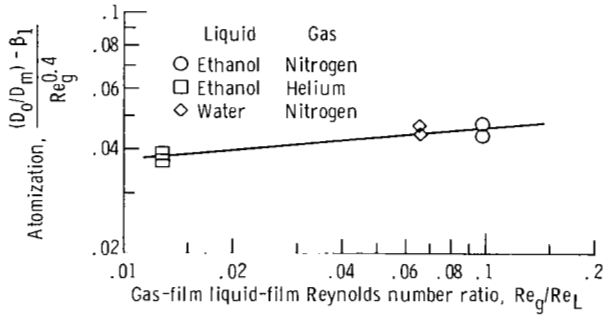

Figure 8. - Effect of ratio of gas-film to liquid-film Reynolds numbers on atomization, Orifice diameter, 0.025 centimeter; slope, 0.1.

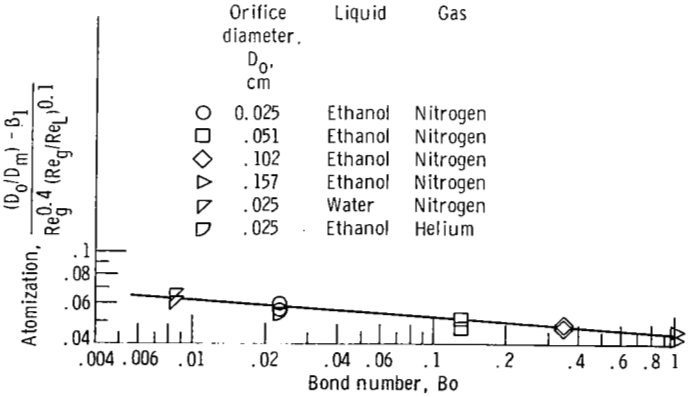

Figure 9. - Effect of Bond number on atomization when velocity difference is negligible. Slope, -0.07.

$$\frac{D_o}{D_m} = \beta_1 + 0.044\ Re_g^{0.5} Re_L^{-0.1} Bo^{-0.07} \tag{12}$$

For this condition ($V_g = V_l$), the gas-stream Reynolds number appeared to have the greatest effect on the atomization process.

Gas-stream and liquid-jet velocities are constant and unequal. - This more general condition ($V_g \neq V_l$ and Ac = 0) is of considerable interest in fuel-spray combustion studies. For this condition, equation (12) may be expanded to include the effect of the liquid and gas Weber number as follows:

$$\frac{D_o}{D_m} - \beta_1 - \beta_2 = c Re_g^{m'} Re_L^{n'} We_g^{h} We_L^{k} Bo^{p'} \tag{13}$$

where

$$\beta_2 = 0.044\ Re_g^{0.5} Re_L^{-0.1} Bo^{-0.07}$$

as in equation (12).

Since the five dimensionless groups in equation (13) could not be varied independently, exponents h and k were determined first by assuming m', n', and p' to be equal, respectively, to m, n, and p of equation (11). The data plotted in figures 10 and 11 show

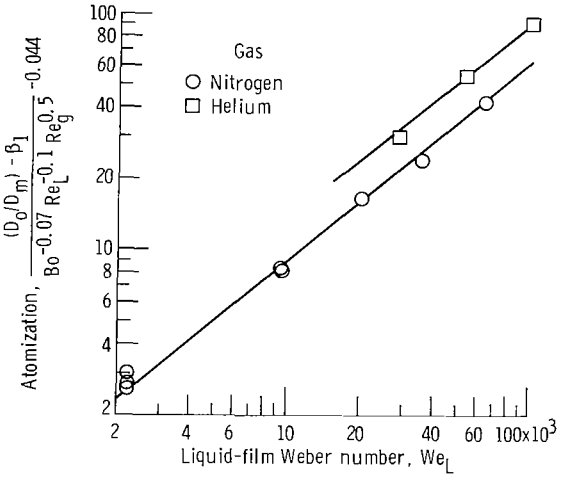

Figure 10. - Effect of liquid-film Weber number on atomization, with gas-film Weber number varying. Slope, 0.8; orifice diameter, 0.025 centimeter; liquid, ethanol.

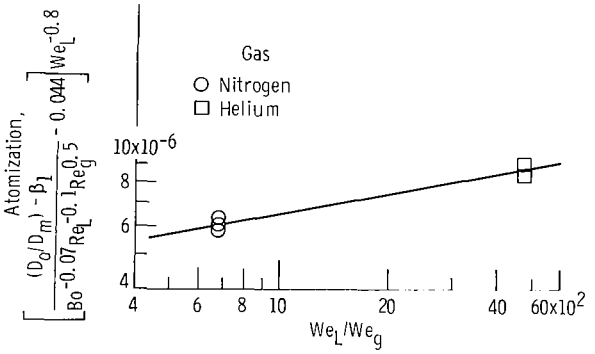

Figure 11. - Effect of ratio of liquid-film to gas-film Weber number on atomization. Slope, 0.2; orifice diameter, 0.025 centimeter; liquid, ethanol.

the following relations:

$$\left(\frac{D_o}{D_m} - \beta_1 - \beta_2\right)\left(Re_g^{-0.5} Re_L^{0.1} Bo^{0.07}\right) \sim We_L^{0.8}$$

in figure 10, when We_L/We_g was constant, and

$$\left(\frac{D_o}{D_m} - \beta_1 - \beta_2\right)\left(Re_g^{-0.5} Re_L^{0.1} Bo^{0.07}\right) \sim We_L^{0.8}\left(\frac{We_L}{We_g}\right)^{0.2} \sim We_L We_g^{-0.2}$$

in figure 11, when We_L/We_g was varied.

Additional data showed that this relation did not correctly account for the effect of different orifice diameters. However, it was found that the orifice diameter dependency could be adequately evaluated by changing the exponent on the Bond number. Thus, as shown in figure 12, a new value for this exponent was determined as well as the value for the proportionality constant c in equation (13). This gave the following expression for equation (13)

$$\frac{D_o}{D_m} - \beta_1 - \beta_2 = 1.25\times10^{-6}\, Re_L^{-0.1} Re_g^{0.5} We_L We_g^{-0.2} Bo^{-0.14} \qquad (14)$$

For this more general condition of liquid-jet atomization, the maximum drop-diameter appeared to be effected more by changes in the liquid-jet Weber number than by variations of the gas-stream Weber number.

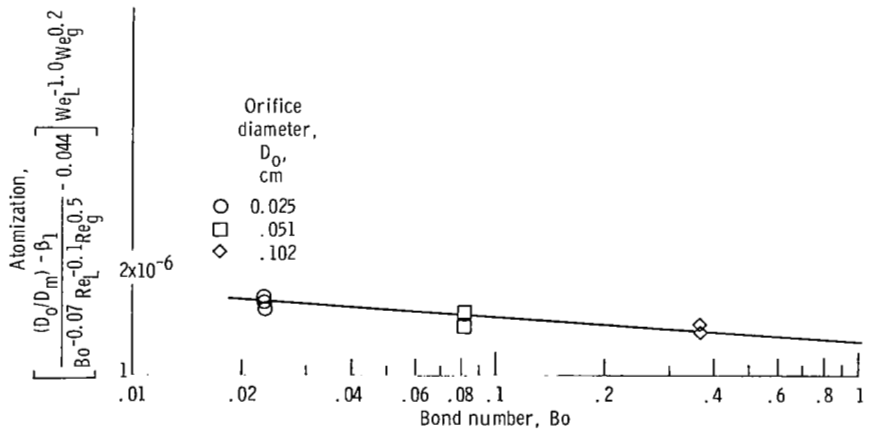

Figure 12. - Effect of Bond number on atomization when velocity difference is relatively high. Slope, -0.07; liquid, ethanol; gas, helium.

Gas-stream is accelerating or decelerating. - This condition ($Ac \neq 0$) is also of considerable interest in fuel-spray combustion studies. For this condition, equation (14) may be expanded to include the effect of the aerodynamic-acceleration group Ac on the maximum drop-diameter as follows:

$$\frac{D_o}{D_m} - \beta_1 - \beta_2 - \beta_3 = d Re_g^{m''} Re_L^{n''} We_g^{h'} We_L^{k'} Bo^{p''} Ac^{q} \tag{15}$$

where

$$\beta_3 = 1.25\times10^{-6}\, Re_L^{-0.1} Re_g^{0.5} We_L We_g^{-0.2} Bo^{-0.14}$$

as in equation (14).

Since it was difficult to independently vary the dimensionless groups in equation (15), it was assumed that the exponents for Re_g, Re_L, We_g, We_L, and Bo would remain the same for this condition as those given in equation (14). This gave the following relation:

$$\frac{\frac{D_o}{D_m} - \beta_1 - \beta_2 - \beta_3}{Re_L^{-0.1} Re_g^{0.5} We_L We_g^{-0.2} Bo^{-0.14}} \sim Ac^{q}$$

The value for the exponent q was determined from a plot of this relation, as shown in figure 13. However, it showed that the relation would not give a correlation for the different orifice diameters. Thus, the data was plotted as shown in figure 14, and a correlation was obtained between the maximum drop-diameter data and all of the dimensionless groups used in this study. From this data plot, the value for the exponent on the Bond number was determined, and the assumption that the exponents for Re_g, Re_L, We_L, and We_g were unchanged for the condition of accelerating or decelerating gas streams produced a good correlation with the experimental data. As a result, it was found that the aerodynamic-acceleration group Ac could be correlated with the maximum drop-diameter data for both accelerating and decelerating gas streams, when a was defined as the absolute acceleration of the gas stream.

From figure 14, it was also possible to determine the value for the proportionality constant d in equation (15). Thus, from figures 13 and 14, it was possible to rewrite equation (15) as follows:

$$\frac{D_o}{D_m} = \beta_1 + \beta_2 + \beta_3 + 3.5\times10^{-7}\, Re^{-0.1} Re_g^{0.5} We_L We_g^{-0.2} Ac^{0.5} Bo^{-0.8} \tag{16}$$

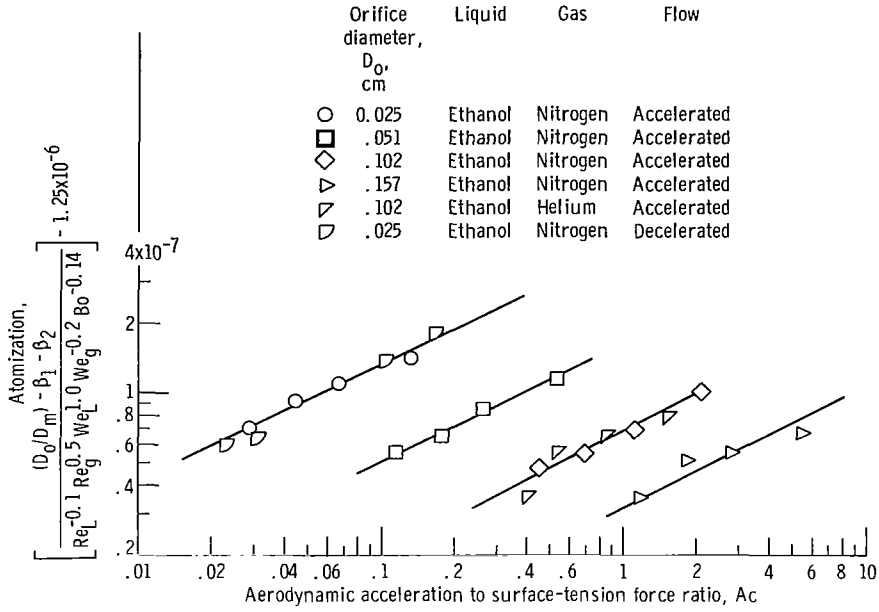

Figure 13. - Effect of the acceleration of the gas-stream on atomization. Slope, 0.5.

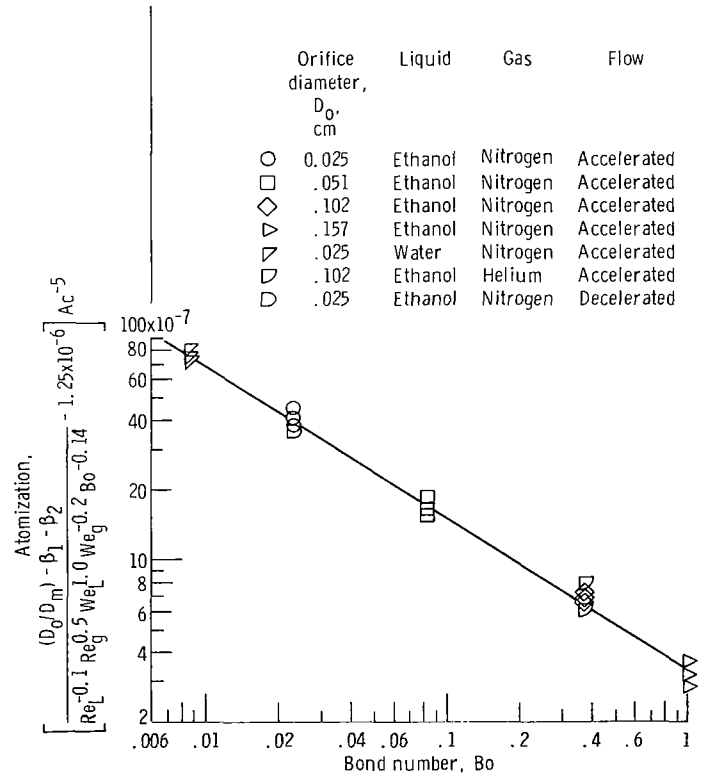

Figure 14. - Effect of Bond number on atomization in an accelerating or decelerating gas stream. Slope, -0.66.

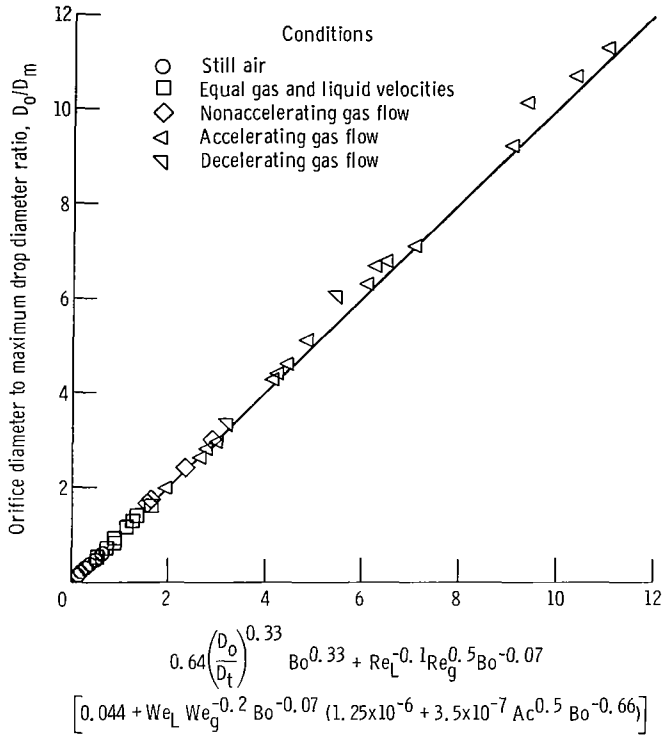

Figure 15. - Correlation of maximum drop diameter with dimensionless groups.

This expression shows that accelerating or decelerating the gas stream will have considerable effect on the maximum drop-diameter particularly when the Bond number is small. Also, equation (16) may be simplified by rewriting it as follows:

$$\frac{D_o}{D_m} = 0.64\left(\frac{D_o}{D_t}\right)^{0.33} Bo^{0.33} + Re_L^{-0.1} Re_g^{0.5} Bo^{-0.07}$$

$$\times \left[0.044 + We_L We_g^{-0.2} Bo^{-0.09}(1.25\times10^{-6} + 3.5\times10^{-7}\, Ac^{0.5} Bo^{-0.66})\right] \qquad (17)$$

The plot in figure 15 shows fairly good agreement of all of the maximum drop-diameter data with equation (17).

In figure 16, a plot of equation (17) is given to show how the atomization conditions may be viewed as being additive in nature. For example, a pendant drop of ethanol will have a maximum diameter of 0.1800 centimeters when suspended in still air from a tube having an inside diameter of 0.0254 centimeter and an outside diameter of 0.0483 centimeter. When the liquid velocity and the velocity of the surrounding gas are increased

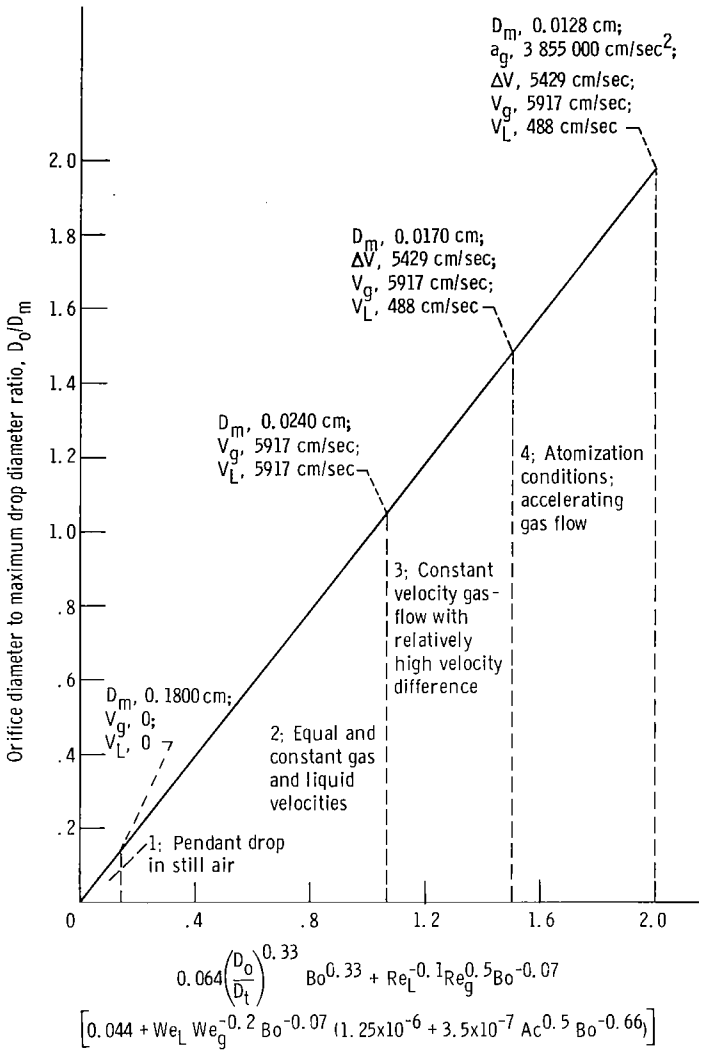

Figure 16. - Effect of accelerating flow of nitrogen gas stream on fineness of atomization of cocurrent ethanol jets. Orifice diameter, 0.025 centimeter.

from approximately 0 up to 5917 centimeters per second, then the maximum drop diameter decreased to 0.0240 centimeter. Decreasing the liquid velocity to 488 centimeters per second, to give a velocity difference of 5429 centimeters per second, produced a further reduction of the maximum drop-diameter to 0.0170 centimeter. Finally, the maximum drop-diameter was reduced to 0.0128 centimeter by accelerating the nitrogen gas stream up to 3 855 000 centimeters per second squared, and maintaining the same velocity difference at the injector orifice. A similar reduction in drop size could have been obtained by increasing the velocity difference.

Comparison of Results with Other Investigations

Several studies have been made regarding the atomization of liquid jets in nonaccelerating gas streams. Weiss and Worsham (ref. 6) determined mass-median drop-diameters which they used to characterize liquid-jet atomization. Thus, their results cannot be compared directly with the results of this study. However, the exponents which they determined for fluid properties and the orifice diameter may be compared to some extent as shown in table III. Similarly, the results of Nukiyama and Tanasawa

TABLE III. - COMPARISON OF RESULTS WITH OTHER INVESTIGATIONS OF LIQUID-JET BREAKUP IN NONACCELERATING GAS STREAMS

Characteristic drop diameter	Exponent for -								
	Orifice diameter, D_o	Differential velocity, ΔV	Liquid-jet velocity, V_l	Gas-stream velocity, V_g	Gas-stream density, ρ_g	Liquid-jet density, ρ_l	Gas-stream viscosity, μ_g	Liquid-jet viscosity, μ_l	Surface tension, σ
Maximum (eq. (14))	0.08	-1.6	0.1	-0.5	-0.3	-0.76	0.5	-0.1	0.66
Mass-median (ref. 6)	.16	-1.33	.08	----	-----	-.84	.09	.34	.41
Sauter (ref. 7)	----	-1.0	----	----	-----	-.5	----	-----	.5

(ref. 7) are shown in table III for the Sauter mean-drop size. The two references do not distinguish between the velocity difference ΔV and the gas-stream velocity so it is difficult to compare exponents for these terms. However, the agreement is fairly good for a number of the fluid properties and the orifice diameter.

CONCLUSIONS

The fineness of atomization of liquid-jets may be characterized by the ratio of the orifice diameter to the maximum drop diameter D_o/D_m. This nondimensional drop-size parameter may be a function of one or as many as six dimensionless groups, depending on the atomization conditions. For the four conditions investigated in this study, this relation is given by the following expression:

$$\frac{D_o}{D_m} = 0.64\left(\frac{D_o}{D_t}\right)^{0.33} Bo^{0.33} + Re_L^{-0.1} Re_g^{0.5} Bo^{-0.07}$$

$$\times \left[0.044 + We_L We_g^{-0.2} Bo^{-0.07}(1.25\times10^{-6} + 0.33\times10^{-6}\, Ac^{0.5} Bo^{-0.67})\right]$$

In considering the acceleration effect of a gas stream, it was found to be an important factor in determining the fineness of atomization of liquid-jets.

Lewis Research Center,
National Aeronautics and Space Administration,
Cleveland, Ohio, February 20, 1968,
128-31-06-02-22.

APPENDIX - SYMBOLS

Ac	aerodynamic-acceleration to surface-tension force ratio based on orifice diameter, $(\rho_g D_o^2 a/\sigma)$
a	absolute gas-stream acceleration, cm/sec^2
Bo	hydrostatic to surface-tension force ratio, based on orifice diameter, $(\rho_l D_o^2 g/\sigma)$
b, c, d	constants in equations (11), (13), and (15), respectively
D_m	maximum observed drop diameter, cm
D_o	orifice diameter, cm
g	gravitational acceleration, cm/sec^2
h, k, m, n, p	exponents in equations (11), (13), and (15), respectively
Re_g	Reynolds number for gas, based on orifice diameter, $(D_o \rho_g V_g/\mu_g)$
Re_L	Reynolds number for liquid based on orifice diameter, $(D_o \rho_l V_l/\mu_l)$
V	velocity, cm/sec
ΔV	relative velocity of gas stream with respect to liquid-jet velocity, $(V_g - V_l)$, cm/sec
We_g	Weber number for gas based on orifice diameter, $(\rho_g D_o (\Delta V)^2/\sigma)$
We_L	Weber number for liquid based on orifice diameter, $(\rho_l D_o (\Delta V)^2/\sigma)$
x	downstream distance in accelerated flow duct, cm
$\beta_1, \beta_2, \beta_3$	constants defined in equations (10), (12), and (14), respectively
μ	viscosity, $N\text{-}sec/m^2$
ρ	density, g/cm^3
σ	surface tension, N/cm
ψ	constant (eq. (9))
Subscripts:	
g	gas stream
L	liquid jet
m	maximum
o	orifice
t	tip

REFERENCES

1. Ingebo, Robert D.; and Foster, Hampton, H.: Drop-Size Distribution for Cross-current Breakup of Liquid Jets in Airstreams. NACA TN 4087, 1957.

2. Priem, Richard J.; and Heidmann, Marcus F.: Vaporization of Propellants in Rocket Engines. ARS J., vol. 29, no. 11, Nov. 1959, pp. 836-842.

3. Ingebo, Robert D.: Heat-Transfer and Drag Coefficients for Ethanol Drops in a Rocket Chamber Burning Ethanol and Liquid Oxygen. Eighth Symposium (Internation) on Combustion. The Williams and Wilkins Co., 1962, pp. 1104-1113.

4. Ingebo, Robert D.: Photomicrographic Tracking of Ethanol Drops in a Rocket Chamber Burning Ethanol and Liquid Oxygen. NASA TN D-290, 1960.

5. Hersch, Martin; and Rice, Edward J.: Gaseous-Hydrogen - Liquid-Oxygen Rocket Combustion at Supercritical Chamber Pressures. NASA TN D-4172, 1967, p. 16.

6. Weiss, Malcolm A.; and Worsham, Charles H.: Atomization in High Velocity Airstreams. ARS J., vol. 29, no. 4, Apr. 1959, pp. 252-259.

7. Nukiyama, Shiro; and Tanasawa, Yasusi (E. Hope, trans.): Experiments on the Atomization of Liquids in Airstreams. Rep. No. 3, On the Droplet-Size Distribution in an Atomized Jet. Defense Res. Board, Dept. Nat. Defense, Ottawa (Canada), Mar. 18, 1950; (Trans. from Trans. Soc. Mech. Engr. (Japan), vol. 5, no. 18, Feb. 1939, pp. 62-67).

8. Richardson, Edward G.: Dynamics of Real Fluids. Arnold and Company, London, 1950, p. 105.

9. Harkins, William D.; and Brown, F. E.: The Determination of Surface Tension (Free Surface Energy), and the Weight of Falling Drops: The Surface Tension of Water and Benzene by the Capillary Height Method. J. Am. Chem. Soc., vol. 41, no. 4, Apr. 1919, pp. 499-524.

NASA-Langley, 1968 —— 12 E-4325